Nonlinear optical pulse transformations in fibre-based systems

Sonia Boscolo and Sergei K. Turitsyn

Photonics Research Group,
School of Engineering and Applied Science, Aston University,
Birmingham B4 7ET, United Kingdom

OUTLINE

- Autosolitons in high-speed fibre communication systems
- Parabolic pulse generation and characterization
- Passive nonlinear pulse shaping in normally dispersive fibre systems
- Applications of parabolic/flat-top pulses
- Applications of triangular pulses
- Summary

Acknowledgements

A. I. Latkin, R. S. Bhamber, A. S. Kovalev, M. M. Bogdan, S. A. Derevyanko, I. O. Nasieva, A. A. Sysoliatin, A. Yu. Plocky, V. F. Khopin, P. Harper, J. Harrison.

THE MODEL. Pulse evolution in a cascaded transmission system with periodic dispersion and nonlinearity variations, frequency filtering, and management by nonlinear optical devices (NODs)

$$i\psi_z - \frac{1}{2}\beta_2(z)\psi_{tt} + \sigma(z)|\psi|^2\psi = iG(z,|\psi|^2)\psi,$$

$$G(z,|\psi|^2) = -\gamma(z) + \sum_k \delta(z-kZ_a)\left\{\exp\left[\int_{(k-1)Z_a}^{kZa} \mathrm{d}z\,\gamma(z)\right] - 1\right\}$$
$$+\sum_k \delta(z-kZ_f)[h(t) * -1] + \sum_k \delta(z-kZ_0)[f(|\psi|^2)-1].$$

– $\psi(z,t)$: pulse envelope in comoving coordinates,
$\beta_2(z)$: varying fibre group-velocity dispersion (GVD) parameter, σ: nonlinearity parameter,
Z_a, Z_f, Z_0: amplifier, filter, and NOD insertion periods,
γ: fibre loss coefficient, $\exp[\int_{(k-1)Z_a}^{kZ_a} \mathrm{d}z\,\gamma(z)] - 1$: amplification coefficient,
$h(t) = \mathcal{F}^{-1}[\tilde{h}(\omega)]$, $\mathcal{F}^{-1}$: inverse Furier transform, $\tilde{h}(\omega)$: filter transfer function, $*$: Fourier convolution,
$f(P)$: NOD power-dependent transfer function.

- Case of linear propagation in fibre: $L_{NL} = (\sigma P_0)^{-1} \gg L_D = T^2/|\beta_2|$
(P_0: signal peak power, T: pulse width).

SIGNAL MAP – transmission line element comprising a NOD, a piece of linear fibre of length Z_0 and m filters

$$\exp(i\mu)U_{n+1}(t) = \int_{-\infty}^{\infty} \mathrm{d}t'\, K(t-t';Z_0)f(|U_n(t')|^2)U_n(t'), \qquad n = 0, 1, \ldots$$

where

$$K(t-t';Z_0) = \frac{1}{2\pi}\int_{-\infty}^{\infty} \mathrm{d}t''\, H(t-t'-t'')F(t'';Z_0),$$

$$H(t) = \mathcal{F}^{-1}[\tilde{h}^m(\omega)], \qquad F(t;Z_0) = \sqrt{i/B_0}\exp(-it^2/(2B_0)), \qquad B_0 = \int_{nZ_0}^{(n+1)Z_0} \mathrm{d}z\, \beta_2(z).$$

– $U(z,t) = Q^{-1}(z)\psi(z,t)$,
$Q(z) = \exp[-\int_{(k-1)Z_a}^{z} \mathrm{d}z'\, \gamma(z')]$ for $(k-1)Z_a < z < kZ_a$, $Q(z) = 1$ for $z = kZ_a^+$,
NOD placed immediately after amplifier, signal taken at $z = nZ_0^-$.

S. Boscolo et al., Theor. Math. Phys. 144, 1117 (2005); Phys. Rev. E 72, 016601 (2005).

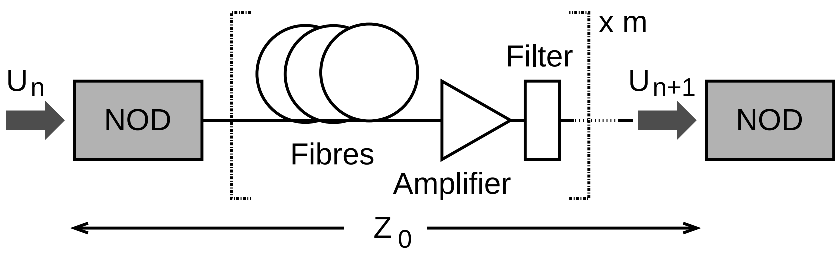

$$U_{n+1}(t) = U_n(t) = U(t) \Rightarrow \text{Steady states } U(t).$$

Autosoliton solutions

$$f(P) = a\sin(bP)\exp(icP), \quad a, b, c \in \Re^{+}$$ nonlinear optical loop mirror (NOLM).

Steady-state acquisition

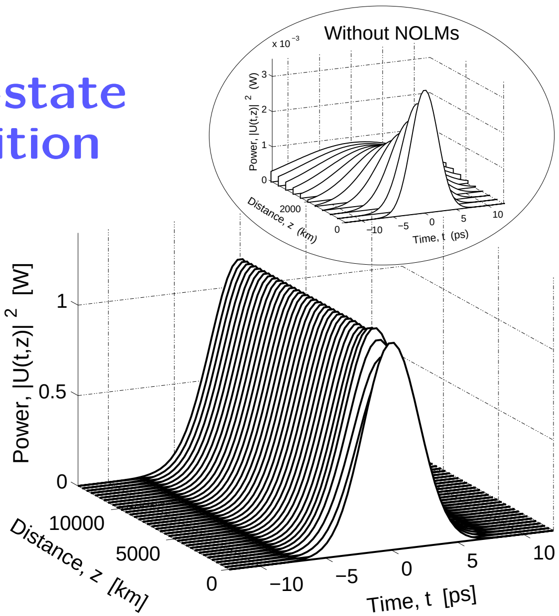

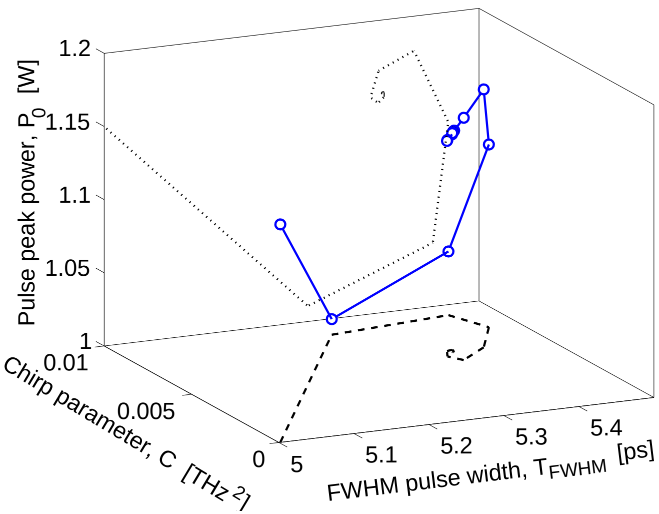

Basin of attraction

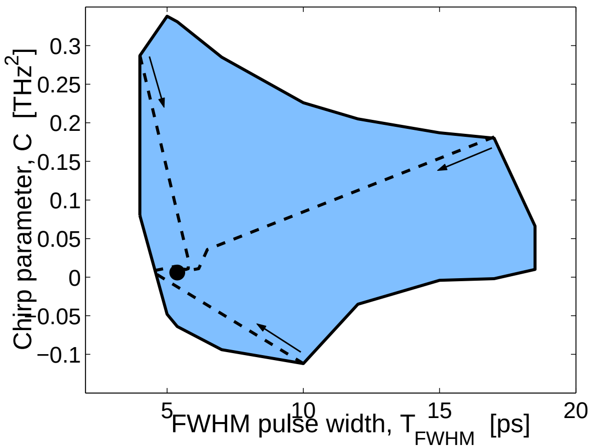

- NLSE numerical integration.
- $m = 1$, $\tilde{h}(\omega) = \exp(-\omega^2/(2\Omega_f^2))$.
- $\langle D \rangle = -2\pi c \langle \beta_2 \rangle / \lambda_0$, $\delta\nu_f = \sqrt{\ln 2}\,\Omega_f/\pi$.

S. Boscolo et al., Phys. Rev. E (2005).

Tolerance to system parameters

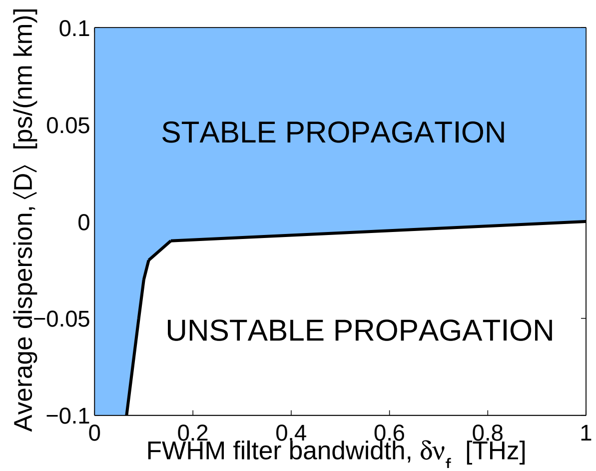

Autosolitons in high-speed fibre communication systems. Approximate mapping

VARIATIONAL MODEL

$$U_n(t) = \sqrt{P_0}\,\exp(-t^2/(4T_{RMS}^2) + iC_{RMS}t^2)$$

– T_{RMS}, C_{RMS}: root-mean-square (RMS) width and chirp parameter.

Output signal parameters = input signal parameters

$$\Downarrow$$

$$P_0 = \frac{1}{\sqrt{2\pi}T_{RMS}}\int_{-\infty}^{\infty}\mathrm{d}t\,|U_{n+1}(t;P_0,T_{RMS},C_{RMS})|^2, \quad T_{RMS}^2 = \frac{\int_{-\infty}^{\infty}\mathrm{d}t\,t^2|U_{n+1}(t;P_0,T_{RMS},C_{RMS})|^2}{\int_{-\infty}^{\infty}\mathrm{d}t\,|U_{n+1}(t;P_0,T_{RMS},C_{RMS})|^2},$$

$$C_{RMS} = \frac{\mathrm{Im}\int_{-\infty}^{\infty}\mathrm{d}t\,U_{n+1}^2(t;P_0,T_{RMS},C_{RMS})(\partial_t U_{n+1}^*(t;P_0,T_{RMS},C_{RMS}))^2}{\int_{-\infty}^{\infty}\mathrm{d}t\,|U_{n+1}(t;P_0,T_{RMS},C_{RMS})|^4}.$$

Steady-state pulse characteristics

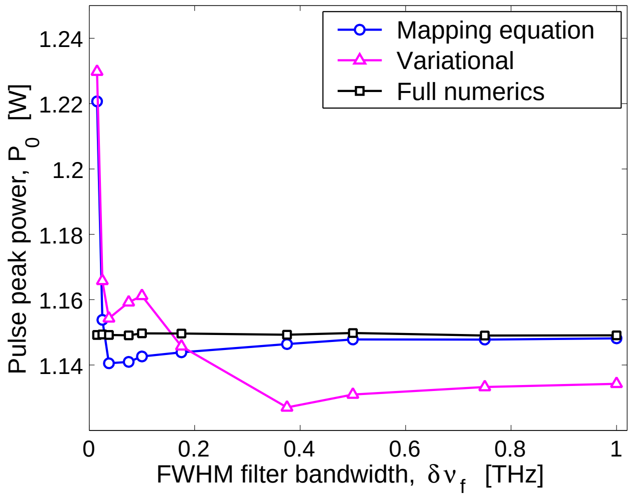

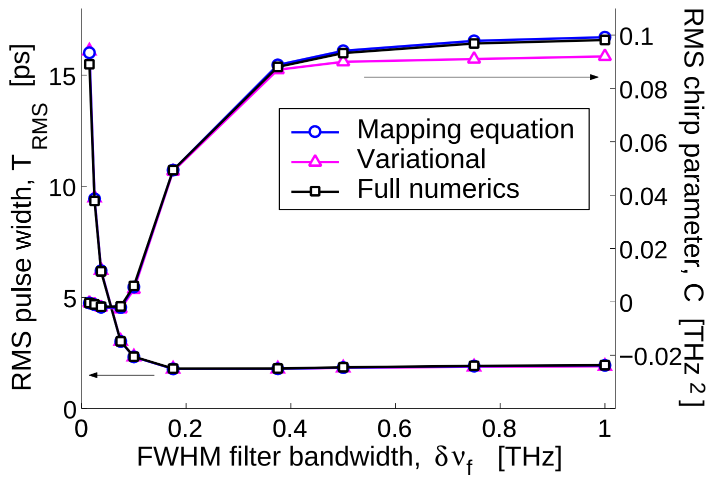

S. Boscolo et al.,
Theor. Math. Phys. (2005).

Aston University PHOTONICS GROUP

Aston University Birmingham

THE MODEL. Pulse evolution in a normally dispersive (ND) fibre gain medium

$$i\psi_z - \frac{\beta_2}{2}\psi_{tt} + \sigma|\psi|^2\psi = i\frac{g(z)}{2}\psi.$$

(+ higher-order terms – Raman, third-order dispersion,. . .)

– $\beta_2 > 0$, σ: GVD and nonlinearity parameters, $g(z)$: gain profile along the fibre.

- Semiclassical limit (large amplitude/small dispersion): $\dfrac{\beta_2|(|\psi|)_{tt}|}{2\sigma|\psi|^3} \ll 1.$

HIGH-INTENSITY SOLUTIONS

$$|\psi(z,t)| = [3\epsilon(z)/(4\tau(z))]^{1/2}\left[1-(t/\tau(z))^2\right]^{1/2}\theta(\tau(z)-|t|),$$

$$\arg\psi(z,t) = \lambda\eta(z) + C(z)t^2,$$

$$\eta(z) = \eta(z_0) + (3\sigma/(4\lambda))\int_{z_0}^{z} \mathrm{d}s\,\frac{\epsilon(s)}{\tau(s)}, \qquad C(z) = -(2\beta_2)^{-1}(\ln\tau(z))_z,$$

$$\epsilon(z) = \epsilon(z_0)\exp\int_{z_0}^{z}\mathrm{d}s\,g(s), \qquad \tau_{zz} = 3\beta_2\sigma\epsilon(z)/(2\tau^2).$$

- D. Anderson et al., J. Opt. Soc. Am. B 10, 1185 (1993).
- M. E. Fermann et al., Phys. Rev. Lett. 84, 6010 (2000).
- S. Boscolo et al., Theor. Math. Phys. 133, 1647 (2002).

Parabolic pulse generation and characterization. What are parabolic pulses?

- *Parabolic intensity profile, linear frequency chirp.*
- *Self-similar* (SS) propagation – scaling between peak amplitude, $\tau(z)$ and $C(z)$.
- Resistance to optical wave-breaking.

Similariton characteristics

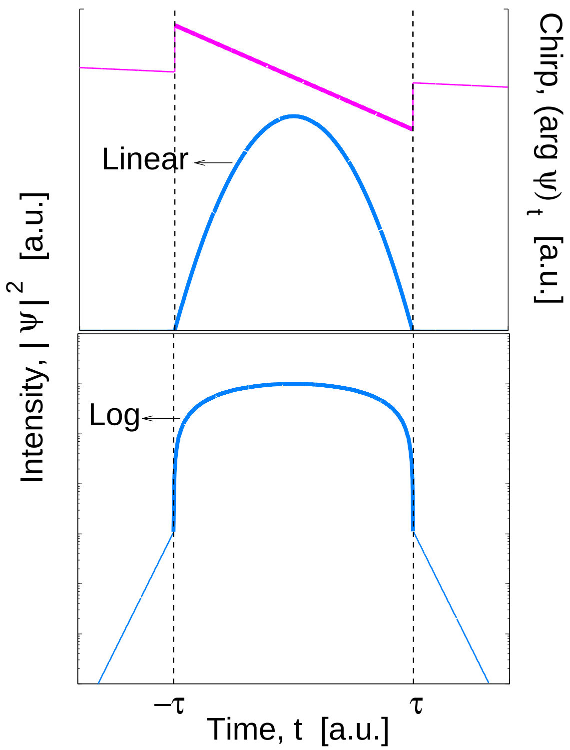

Self-similar evolution

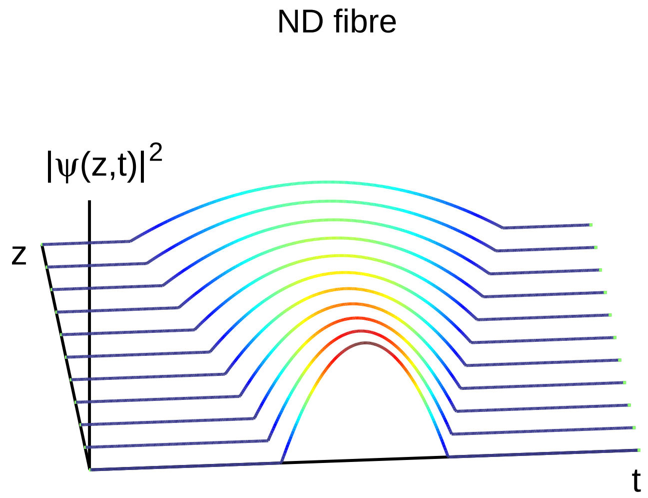

Anderson et al. (1993)
(theory)

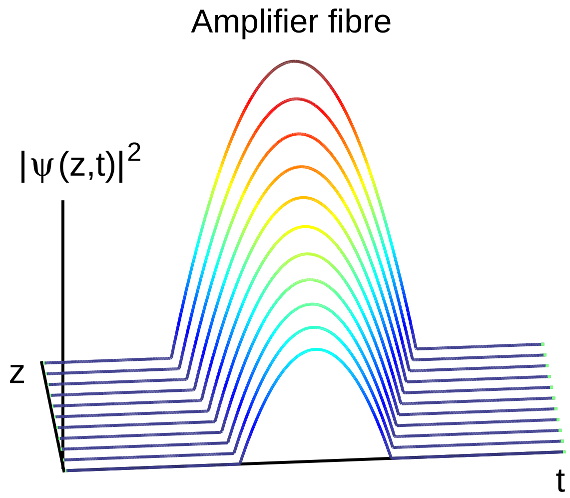

Fermann et al. (2000)
(theory and exper.)

What are parabolic pulses?

- In an idealized amplifier fibre, SS parabolic pulse: *Nonlinear "attractor"* towards which an arbitrarily shaped input pulse of given, sufficiently high energy converges with sufficient distance.

- V. I. Kruglov et al., J. Opt. Soc. Am. B 23, 2541 (2006).
- J. M. Dudley et al., Nat. Phys. 3, 507 (2007).

Pulse reshaping in amplifier

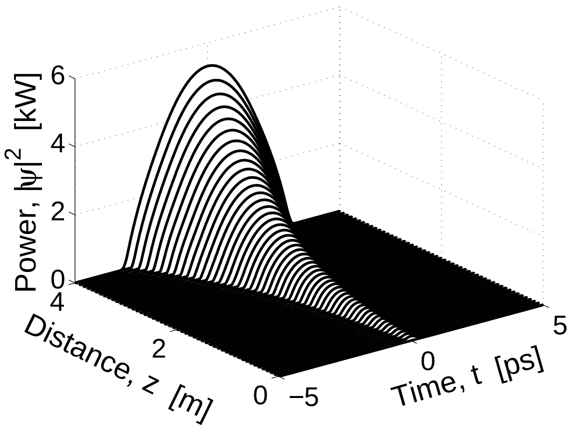

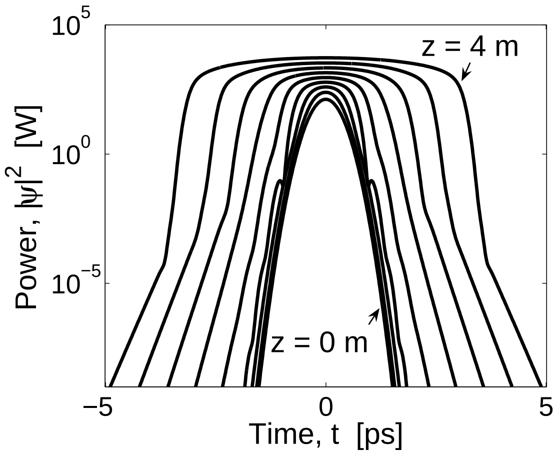

S. Boscolo et al., Theor. Math. Phys. (2002).

Asymptotic solution

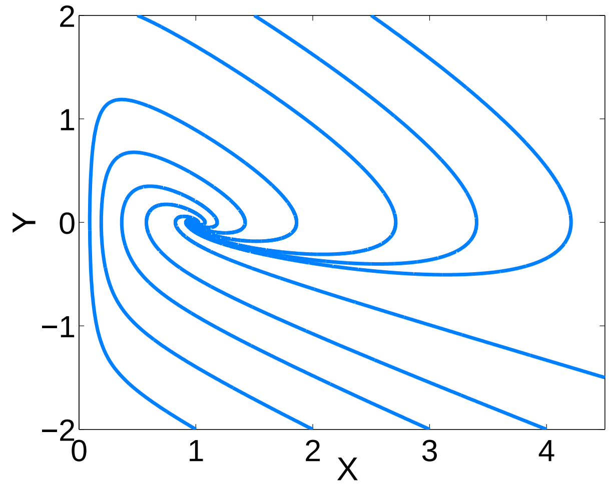

$$X_T = Y, \quad Y_T = -2Y/3 - (X - 1/X^2)/9.$$

– $g(z) = g_0 \neq 0$. $\quad T = g_0 z$, $X = q/q_0$,
$\tau(z) = q(z)\exp(g_0 z/3)$, $q_0 = 3(\beta_2\sigma\epsilon(0)/(2g_0^2))^{1/3}$.

Fixed point $(1,0)$: *stable focus* when $g_0 > 0$ (globally stable), *unstable focus* when $g_0 < 0$.

V. I. Kruglov et al., J. Opt. Soc. Am. B (2006).

Parabolic pulse generation and characterization.
Evolution into the parabolic asymptotic regime

PULSE SHAPE CHARACTERIZATION

$$\kappa = \frac{\int_{-\infty}^{\infty} \mathrm{d}t\, t^2 |\psi|^2 \left(\int_{-\infty}^{\infty} \mathrm{d}t\, |\psi|^4\right)^2}{\left(\int_{-\infty}^{\infty} \mathrm{d}t\, |\psi|^2\right)^5}.$$

– $\kappa = 0.0796$ for Gaussian pulse,
  $\kappa = 0.0720$ for parabolic pulse.

A. I. Latkin and S. K. Turitsyn, Proc. ICTON, 259 (2006).

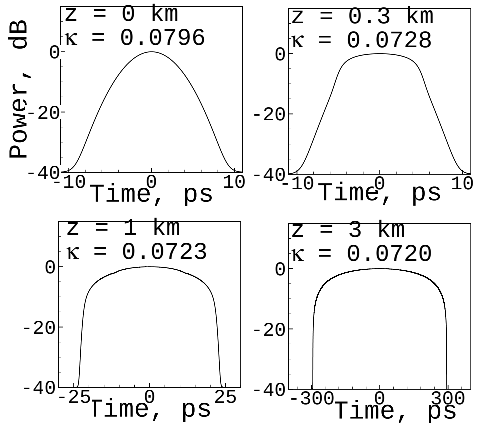

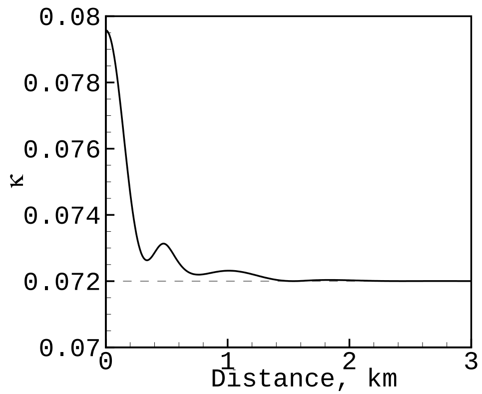

VARIATIONAL APPROACH. Transition from Gaussian to parabolic:

$$u(z,t) = \psi(z,t)\exp\left(-\frac{1}{2}\int_0^s \mathrm{d}s\, g(s)\right)$$

$$= \sqrt{q(z)\exp(-y(z))\ln\left[1+\exp\left(y(z)-t^2/\tau^2(z)\right)\right]}\exp\left[i(\phi(z)+C(z)t^2+B(z)t^4)\right].$$

- Gaussian limit: $|u(z,t)|^2 \to q(z)\exp(-t^2/\tau^2(z))$ when $y(z)\to -\infty$.
- Parabolic limit: $|u(z,t)|^2 \to q(z)\exp(-y(z))\left(y(z)-t^2/\tau^2(z)\right)$ when $y(z)\to +\infty$.

Evolution into the parabolic asymptotic regime

VARIATIONAL APPROACH. Lagrangian equations:

$$y_z = 16\beta_2 B\tau^2 f_y(y), \quad \tau_z = -2\beta_2 C\tau + 4\beta_2 B\tau^3 f_\tau(y),$$
$$C_z = 2\beta_2 C^2 + (\beta_2/(2\tau^4)) f_{C_1}(y) - 8\beta_2 B^2\tau^4 f_{C_2}(y) + (\sigma\epsilon(z)/(4\tau^3)) f_{C_3}(y),$$
$$B_z = 8\beta_2 CB + (\beta_2/(2\tau^6)) f_{B_1}(y) + 8\beta_2 B^2\tau^2 f_{B_2}(y) - (\sigma\epsilon(z)/(4\tau^5)) f_{B_3}(y).$$

– Initial conditions: $y(0) = -y_0$ ($y_0 \gg 1$), $\tau(0) = T_0$, $C(0) = C_0$, $B(0) = 0$ for $\psi(0,t) = \sqrt{P_0}\exp\left(-t^2/(2T_0^2) + iC_0 t^2\right)$.

A. I. Latkin and S. K. Turitsyn, Proc. ICTON (2006).

- Linear dispersive limit: $y \to -\infty$ (with $\sigma = 0$, $g(z) = 0$)

$$\tau_z = -2\beta_2 C\tau, \quad C_z = 2\beta_2 C^2 - \beta_2/(2\tau^4).$$

- Parabolic limit: $y \to +\infty$ (with $B(z \to +\infty) \to 0$, $\tau_P(z) = \tau(z)\sqrt{y(z)}$)

$$(\tau_P)_z = -2\beta_2 C\tau_P, \quad C_z = 2\beta_2 C^2 - 3\sigma\epsilon(z)/(4\tau_P^3) \boxed{+(\beta_2/(2\tau_P^4)) f_{C_1}(y) y^2}, \quad \beta_2 f_{C_1}(y)/(2\tau^4) \propto y^2/\tau_P^4.$$

  - But: Parabolic pulse is a solution only for the central part of the pulse $\Rightarrow$ Integration for $t \in (-\tau\sqrt{y} + \delta, \tau\sqrt{y} - \delta)$ with $0 < \delta \ll 1$ and $\beta_2 f_{C_1}(y)/(2\tau^4) \propto y^2/\tau_P^4 \to 0$ due to $\tau_P(z \to +\infty) \to +\infty$.

Parabolic pulse generation and characterization.
Evolution into the parabolic asymptotic regime

Variational approach vs NLSE simulations

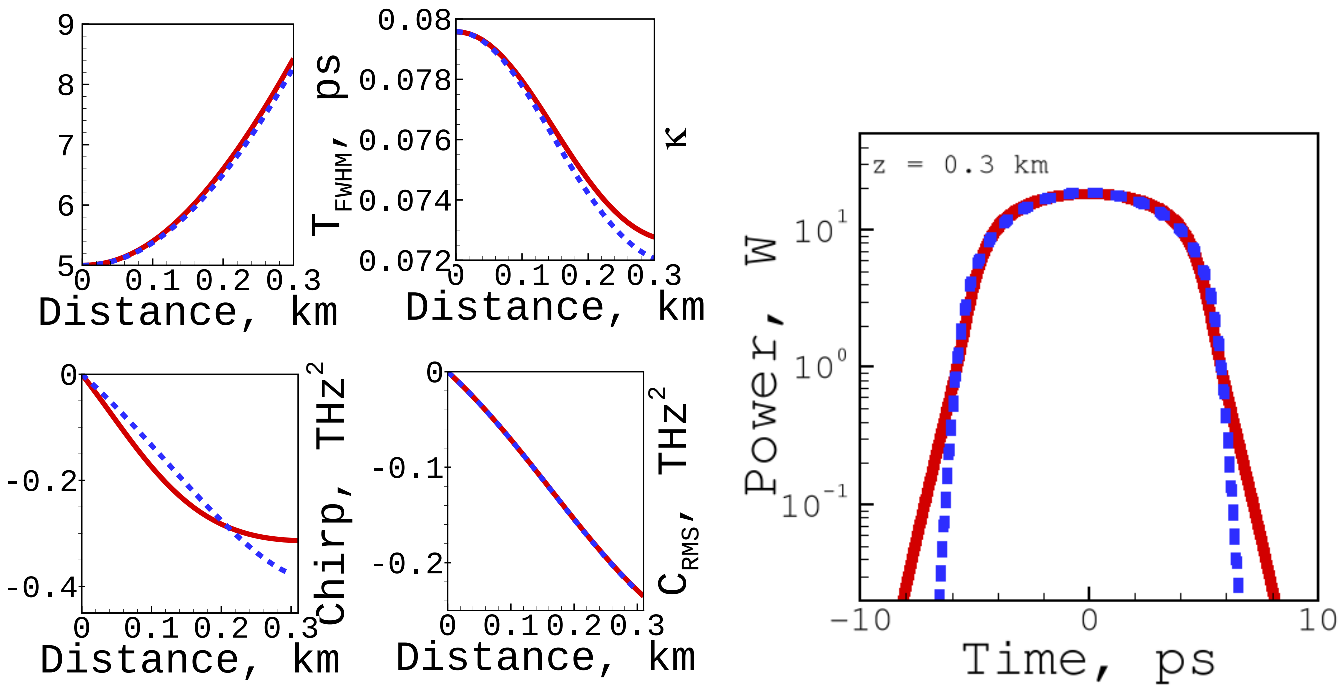

- $\kappa \in (0.073, 0.0796)$.
- $C_{RMS}(z) = i \int \mathrm{d}t\, t(\psi\psi_t^* - \psi^*\psi_t) / \left(4 \int \mathrm{d}t\, t^2|\psi|^2\right)$.

A. I. Latkin and S. K. Turitsyn, Proc. ICTON (2006).

Parabolic pulse generation methods

- Nonlinear reshaping in ND *fibre amplifying media* (rare-earth doped fibres or Raman amplification).

⇒ Good for the generation of high-quality, *high-power* ultrashort pulses.

- K. Tamura and M. Nakazawa, Opt. Lett. 21, 68 (1996).
- M. E. Fermann et al., Phys. Rev. Lett. 84, 6010 (2000).
- C. Finot et al., IEEE J. Sel. Top. Quantum Electron. 10, 1211 (2004).

- Schemes based on *passive fibre* components:
  - Nonlinear reshaping in ND *dispersion-decreasing (DD) fibres*.
  - Linear shaping in *superstructured fibre Bragg gratings*.
  - Nonlinear reshaping in cascaded sections of *ND fibres*.

⇒ Good for applications not requiring high signal power, e.g., *optical telecommunications*.

- T. Hirooka and M. Nakazawa, Opt. Lett. 29, 498 (2004).
- A. Plocky et al., JETP Lett. 85, 319 (2007).
- B. Kibler et al., Electron. Lett. 42, 965 (2006).
- A. I. Latkin et al., Opt. Lett. 32, 331 (2007).
- F. Parmigiani et al., Opt. Express 14, 7617 (2006).
- C. Finot et al., Opt. Express 15, 852 (2007).
- S. Boscolo et al., IEEE J. Quantum Electron. (2008), Submitted.

Parabolic pulses in dispersion-decreasing fibre

A LITTLE BIT OF THEORY. Analogy between active fibre and DD fibre:

$$i\psi_z - \frac{\beta_2}{2} d(z)\psi_{tt} + \sigma|\psi|^2\psi = 0.$$

– $d(z)$: variation in the GVD due to dispersion tapering, $d(0) = 1$.

$$\Updownarrow$$

$$iq_\xi - \frac{\beta_2}{2} q_{tt} + \sigma|q|^2 q = i\frac{g(\xi)}{2} q,$$

$$g(\xi) = -d'(\xi)/d(\xi), \quad \xi = \int_0^z \mathrm{d}s\, d(s), \quad q(\xi,t) = \psi(\xi,t)/\sqrt{d(\xi)}.$$

- $d(z) = 1/(1 + g_0 z) \Rightarrow g(\xi) = g_0$.

T. Hirooka and M. Nakazawa, Opt. Lett. (2004).

Impact of third-order dispersion and loss:

$$iq_\xi - \frac{\beta_2}{2} q_{tt} - i\frac{\beta_3}{6}\exp(g_0\xi) q_{ttt} + \sigma|q|^2 q = \frac{i}{2}\left[g_0 - \alpha\exp(g_0\xi)\right] q.$$

– β_3: TOD coefficient, α: fibre loss coefficient.

- TOD effect grows *exponentially* with distance.
  Effective gain: $g_{eff}(\xi) = g_0 - \alpha\exp(g_0\xi)$. Critical distance: $\xi_0 = \ln(g_0/\alpha)/g_0$ ($L_0 = 1/\alpha - 1/g_0$).

A. I. Latkin et al., Opt. Lett. (2007).

Parabolic pulse generation and characterization.
Parabolic pulses in dispersion-decreasing fibre

Gain effect

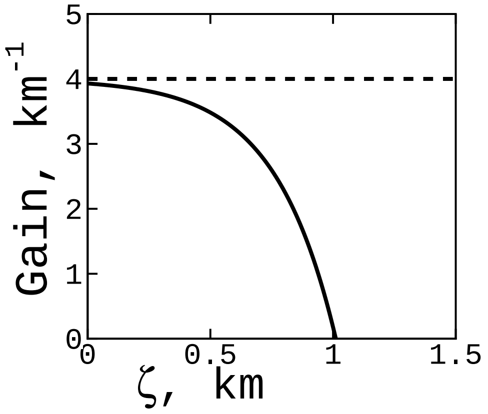

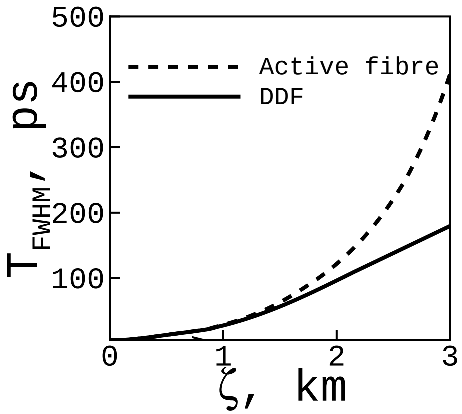

Impact of TOD

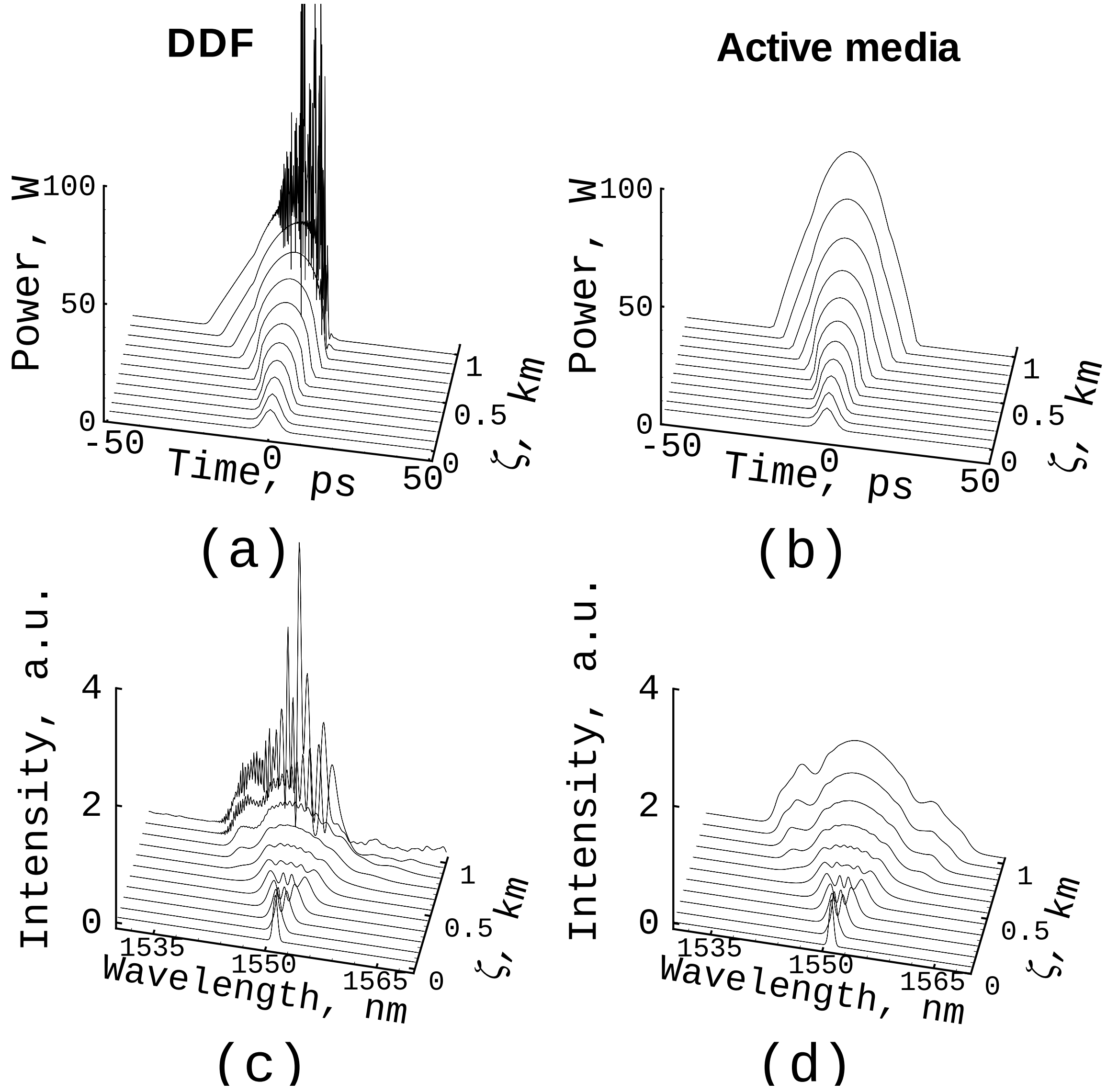

- Limit imposed by the depleting gain effect on the DD fibre length: $\xi_L \leq 1\,\text{km}$ ($L \leq 14\,\text{km}$) for typical fibre parameters.
- Wave breaking due to TOD starts at distances less than $\xi_L \simeq 1\,\text{km}$.

A. I. Latkin et al., Opt. Lett. (2007).

Parabolic pulse generation and characterization.
Parabolic pulses in dispersion-decreasing fibre

Experimental setup

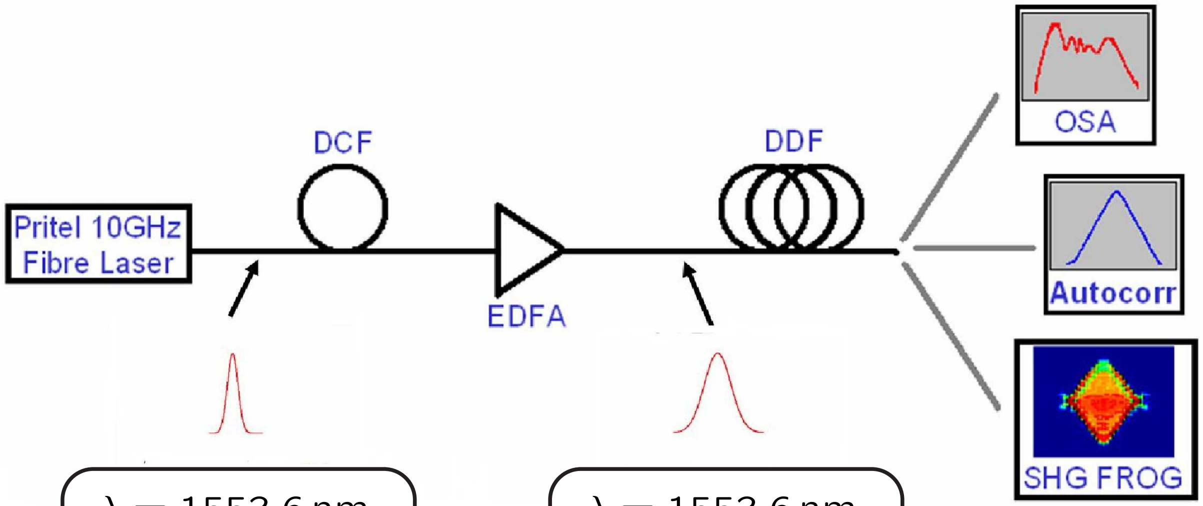

$\lambda = 1553.6\,\text{nm}$
$\Delta\tau = 2.7\,\text{ps}$
$\Delta\lambda = 1.1\,\text{nm}$
$\Delta\tau\Delta\nu = 0.364$

$\lambda = 1553.6\,\text{nm}$
$\Delta\tau = 8.1\,\text{ps}$
$\Delta\lambda = 1.1\,\text{nm}$
$\Delta\tau\Delta\nu = 1.17$

Experimental results: Pulse at the DD fibre input

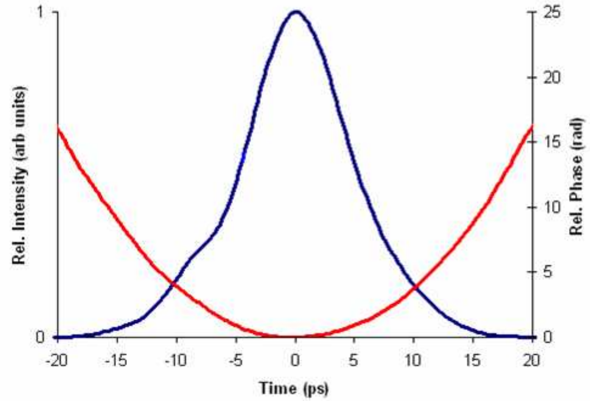

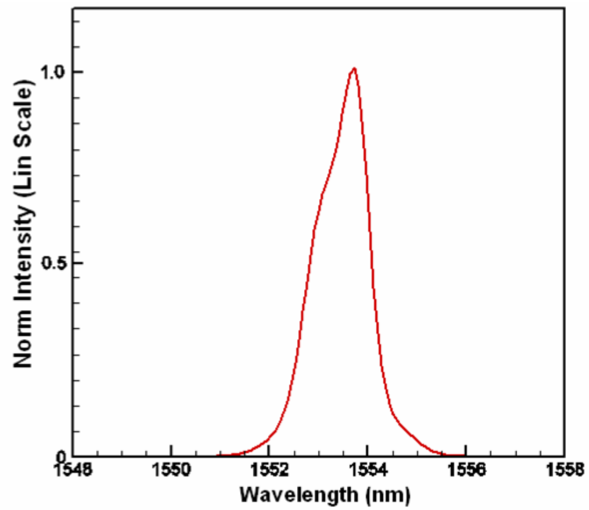

Design DD fibre parameters

$\lambda_0 = 1554\,\text{nm}$, $L = 1050\,\text{km}$
$D(0) = -2\pi c\beta_2/\lambda_0^2 = -2\,\text{ps/(nm km)}$
Dispersion profile:
$\langle D\rangle L = (D(0)/g_0)\ln(1+g_0L) = -1.8\,\text{ps/nm}$
$\beta_3 \sim 0$ at λ_0, $\alpha \sim 0.4\,\text{dB/km}$, $\sigma \sim 2\text{–}3\,(\text{W km})^{-1}$
Diameter: 110–113 μm

A. Yu. Plocky et al., JETP Lett. (2007).

Parabolic pulse generation and characterization.
Parabolic pulses in dispersion-decreasing fibre

Experimental results: Output spectra

Low-power regime

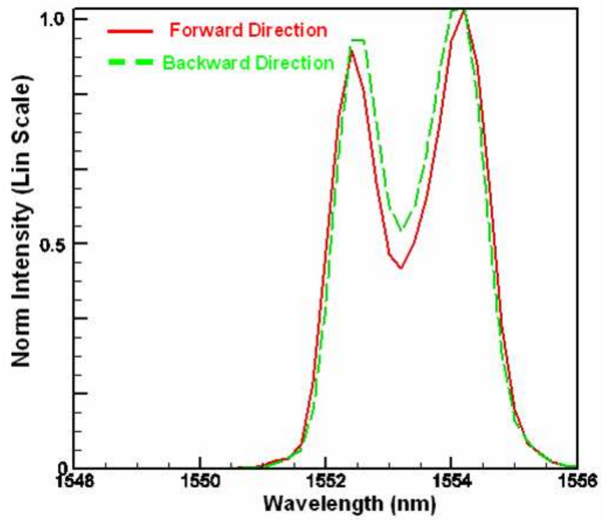

- $P_0 = 1.1\,\mathrm{W}$.
- Similar spectra in both directions.
- Clear evidence of nonlinear broadening.

High-power regime

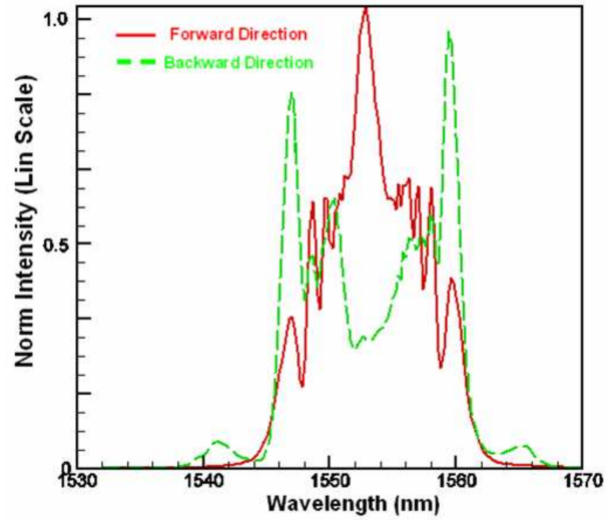

- $P_0 = 22\,\mathrm{W}$.
- Radically different spectra.
- Forward direction shows parabolic pulse spectrum.

Autocorrelations, high-power regime

- Forward direction shows parabolic-like profile:

$$R(t) = ((4/3)\tau - |t| + |t|^3/(12\tau^2))\theta(2\tau - |t|).$$

- Backward direction shows ripples indicative of wave breaking.

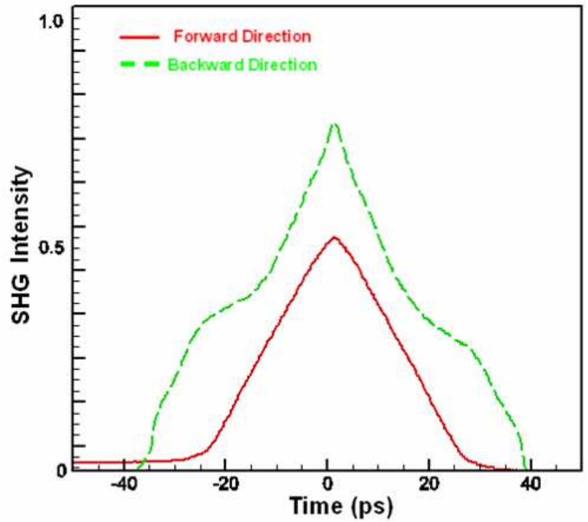

A. Yu. Plocky et al., JETP Lett. (2007).

Optical pulse shaping approaches

- *Spectral amplitude and/or phase linear filtering* in the spatial domain ('Fourier-domain pulse shaping') [ps–fs regimes].

- A. M. Weiner, Prog. Quantum Electron. 19, 161 (1995).

- Integrated *arrayed waveguide gratings* [ps regime].

- T. Kurokawa et al., Electron. Lett. 33, 1890 (1997).

- *Fibre gratings* (fibre Bragg gratings or long-period fibre gratings) [ps–fs regimes].

- P. Petropoulos et al., J. Lightwave Technol. 19, 746 (2001).
- F. Parmigiani et al., J. Lightwave Technol. 24, 357 (2006).
- Y. Park et al., Opt. Express 14, 12670 (2006).

- Temporal coherence synthesization using a *multi-arm interferometer* [ps–fs regimes].

- Y. Park et al., Opt. Express 15, 9584 (2007).

- *Nonlinear effects* in optical fibres [ps–fs regimes].

- C. Finot et al., Opt. Express 15, 852 (2007).
- A. I. Latkin, S. Boscolo, and S. K. Turitsyn, Proc. of OFC, OTuB7 (2008).

Passive nonlinear pulse shaping in normally dispersive fibre systems.
Pulse shaping in a ND fibre

- Pulse *pre-chirping* +
  Nonlinear propagation in a *ND fibre*

$\Downarrow$

Generation of various temporal waveforms of practical interest.

A. I. Latkin et al., Proc. OFC (2008).

Pulse shaper scheme

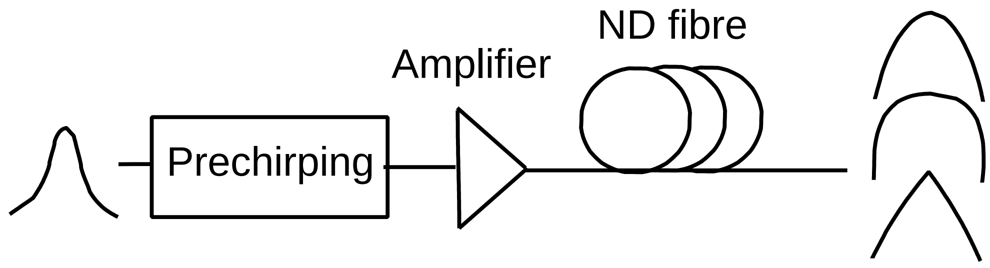

THE MODEL

$$iu_\xi - \frac{1}{2}u_{\tau\tau} + |u|^2 u = 0,$$

where

$$u(\xi,\tau) = NU, \quad U(\xi,\tau) = \psi/\sqrt{P_0}, \quad \xi = z/L_D, \quad \tau = t/T_0,$$
$$L_D = T_0^2/\beta_2, \quad L_{NL} = 1/(\sigma P_0), \quad N = \sqrt{L_D/L_{NL}}.$$

– T_0, P_0: temporal width and peak power of the input pulse,
β_2, σ: GVD and nonlinearity fibre parameters.

Initial pulse: $U(0,\tau) = \exp(-\tau^2/2 + iC\tau^2)$.

– C: normalized chirp parameter.

Pulse shaping in a ND fibre

PULSE SHAPE CHARACTERIZATION. Misfit parameters M_S

$$M_S^2 = \frac{\int_{-\infty}^{\infty} \mathrm{d}\tau \, (|u|^2 - |u_S|^2)^2}{\int_{-\infty}^{\infty} \mathrm{d}\tau \, |u|^4}, \qquad S = FT, P, T,$$

with

$$|u_{FT}(\tau)|^2 = [1 - (\tau/\tau_{FT})^2]^a \theta(\tau_{FT} - |\tau|), \quad 0 < a < 1,$$

$$|u_P(\tau)|^2 = [1 - (\tau/\tau_P)^2]\theta(\tau_P - |\tau|), \quad |u_T(\tau)|^2 = (1 - |\tau/\tau_T|)\theta(\tau_T - |\tau|).$$

– $|u_S|^2$: fits of the same energy and FWHM pulse width.

Reshaping processes

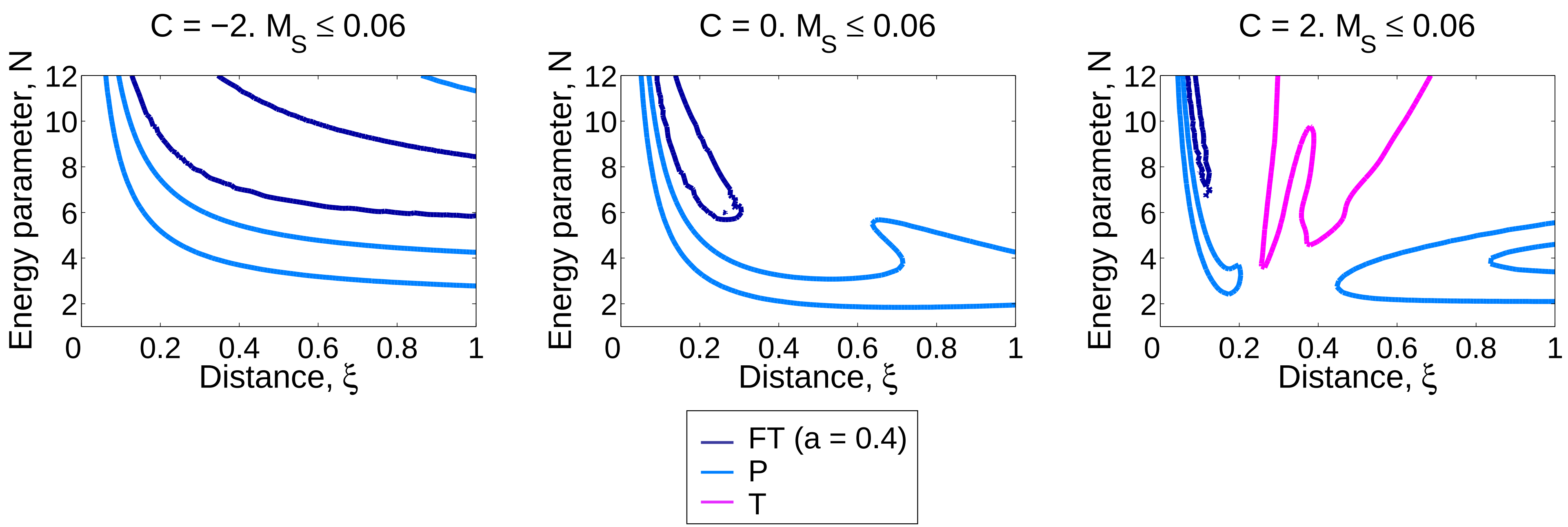

Passive nonlinear pulse shaping in normally dispersive fibre systems.
Pulse shaping in a ND fibre

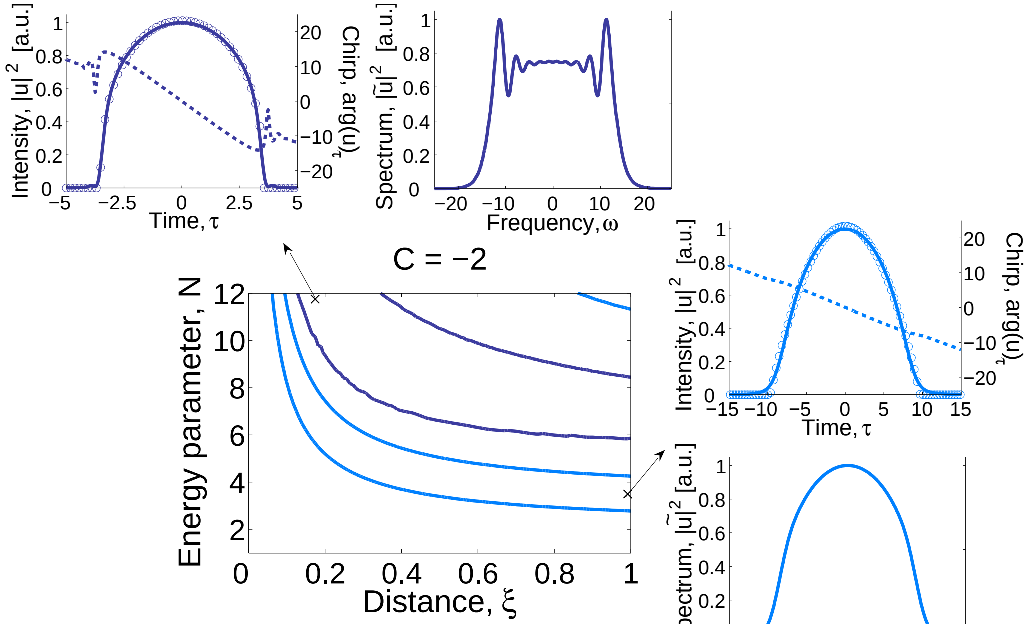

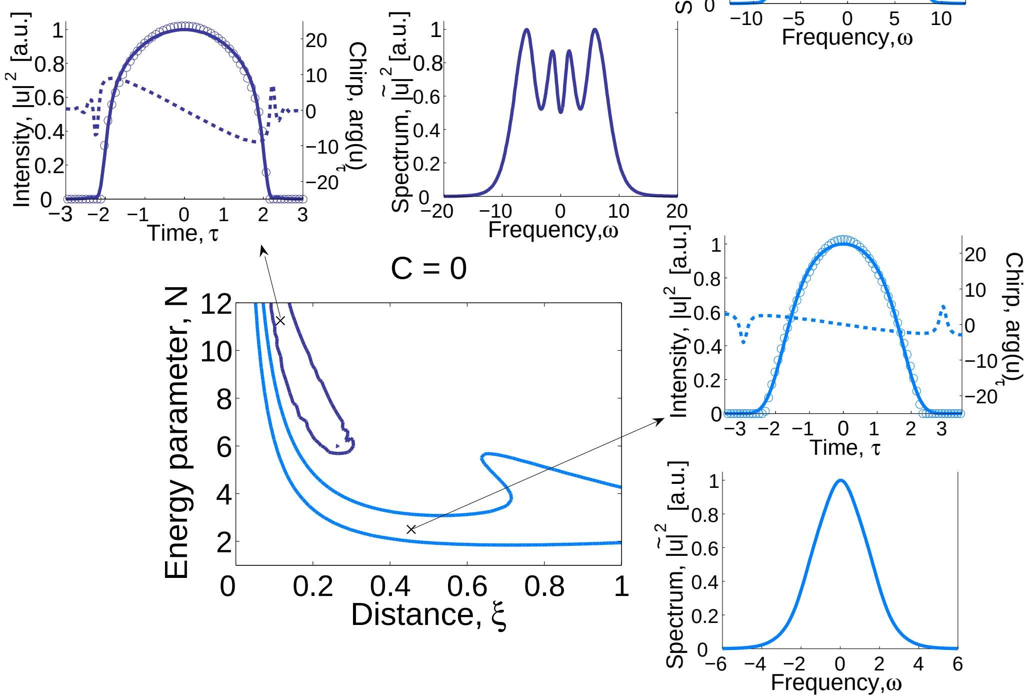

Formed pulses

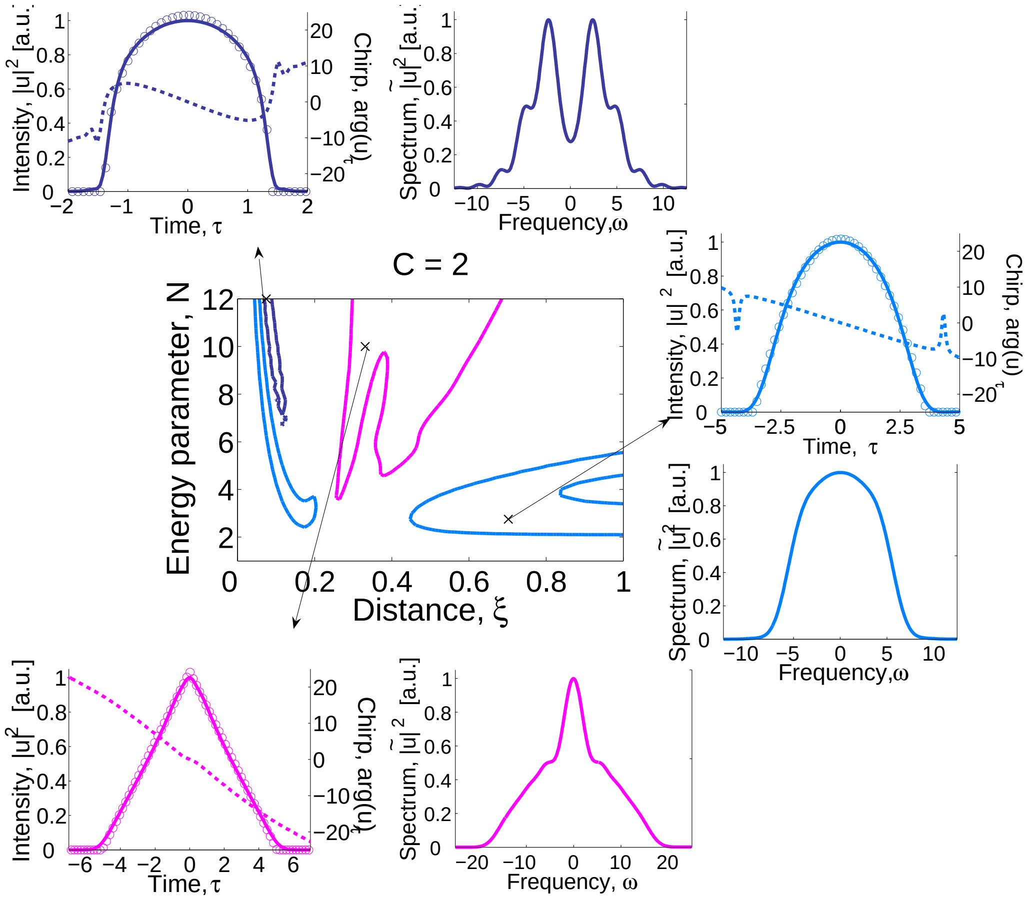

- Best parabolic pulses for moderate N.
- Sufficiently high $N \Rightarrow$ Flat-top pulses.
- Sufficiently high N, $C > 0 \Rightarrow$ Triangular pulses.

Passive nonlinear pulse shaping in normally dispersive fibre systems.
Parabolic pulses in a ND two-segment fibre device

- *Stabilization of the parabolic pulse shape* generated in a ND fibre section by using a *second ND fibre* such that

$$N'/N = b > 1, \quad \text{where} \quad N'^2 = T_0^2\sigma' P_0/\beta_2'.$$

  - β_2', σ': parameters of the second fibre, T_0, P_0: pulse parameters at the input of the first fibre.

C. Finot et al., Opt. Express (2007).

Pulse shaper scheme

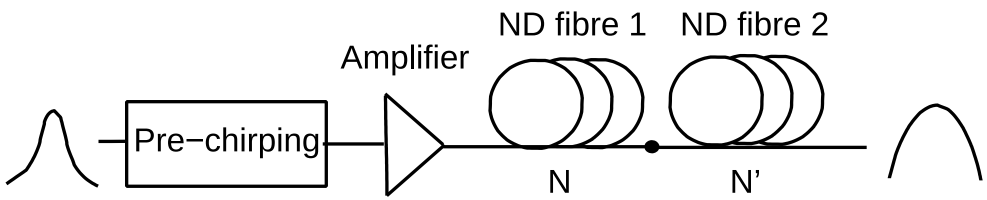

PULSE EVOLUTION CHARACTERIZATION

$$\kappa = \frac{\int_{-\infty}^{\infty} \mathrm{d}\tau\, \tau^2 |u|^2 (\int_{-\infty}^{\infty} \mathrm{d}\tau\, |u|^4)^2}{(\int_{-\infty}^{\infty} \mathrm{d}\tau\, |u|^2)^5}, \qquad \tilde{\kappa} = \frac{\int_{-\infty}^{\infty} \mathrm{d}\omega\, \omega^2 |\tilde{u}|^2 (\int_{-\infty}^{\infty} \mathrm{d}\omega\, |\tilde{u}|^4)^2}{(\int_{-\infty}^{\infty} \mathrm{d}\omega\, |\tilde{u}|^2)^5},$$

$$\Phi = \frac{\int_{-\Delta\tau/2}^{\Delta\tau/2} \mathrm{d}\tau\, ||\phi_{\tau\tau}| - |(\phi_{\tau\tau})_{\tau=0}||}{\int_{-\Delta\tau/2}^{\Delta\tau/2} \mathrm{d}\tau\, |(\phi_{\tau\tau})_{\tau=0}|}.$$

- $\tilde{u}$: Fourier transform of the field envelope, $\phi = \arg u$.

- κ ($\tilde{\kappa}$) $\Rightarrow$ Pulse temporal (spectral) shape.
- Φ $\Rightarrow$ Linearity of the frequency chirp across $\Delta\tau$ around $\tau = 0$ such that $\int_{-\Delta\tau/2}^{\Delta\tau/2} \mathrm{d}\tau\, |u|^2 = a \int_{-\infty}^{\infty} \mathrm{d}\tau\, |u|^2$, $\quad 0 < a \leq 1$.

S. Boscolo et al., IEEE J. Quantum Electron. (2008).

Passive nonlinear pulse shaping in normally dispersive fibre systems.
Parabolic pulses in a ND two-segment fibre device

First-stage pulse evolution, $C = 0$

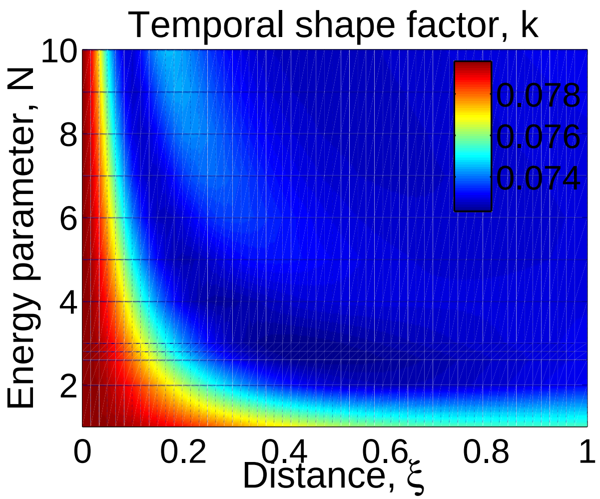

- min(κ) ≈ 0.0723 at ($N_{opt} = 2.8$, $\xi_{opt} = 0.446$), i.e. ($P_0 = 7.4$ W, $z = 54$ m).
- $N' = 3N$, total system length $= 4\,L_D$.
- Second stage starting at (N_{opt}, ξ_{opt}) relative to the first fibre.

Parabolic pulses in the two-stage system

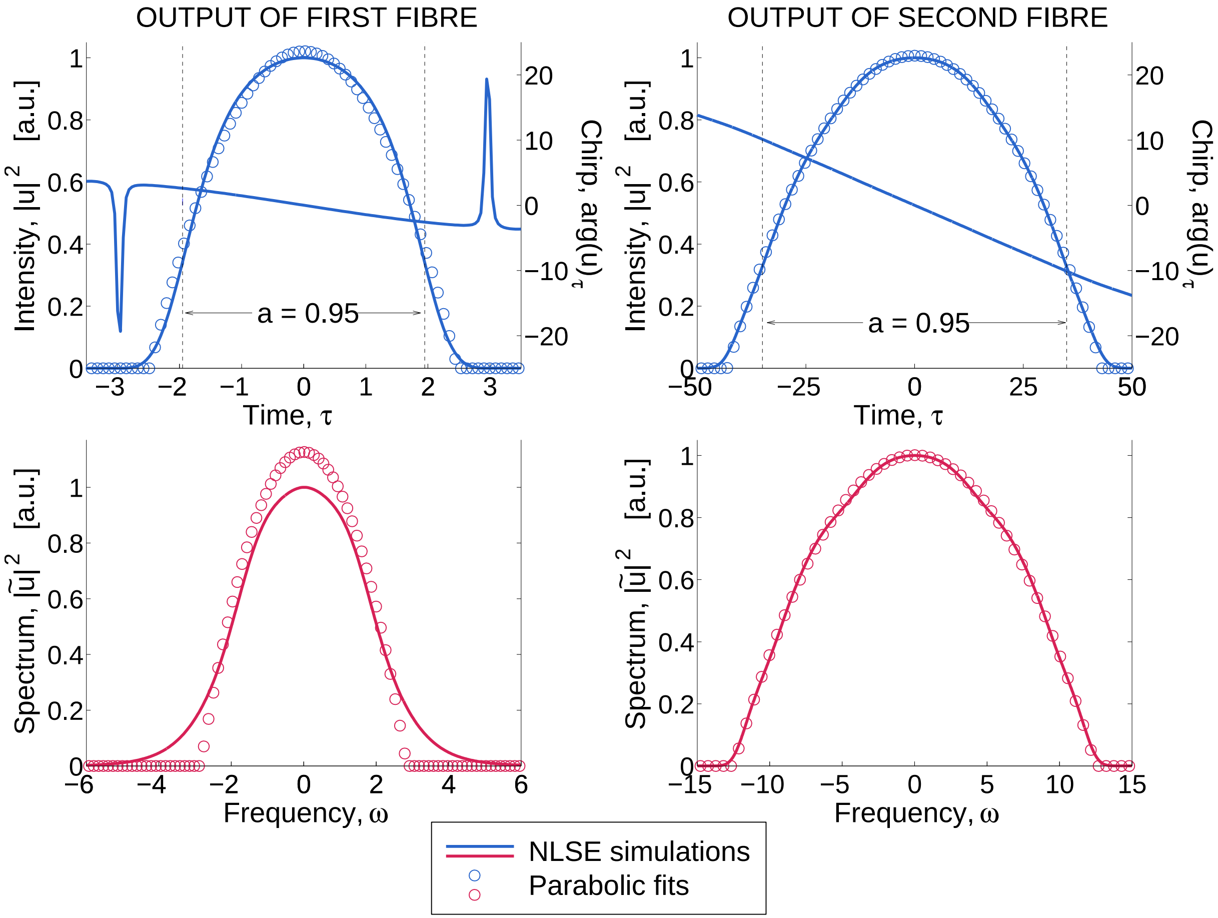

S. Boscolo et al., IEEE J. Quantum Electron. (2008).

Passive nonlinear pulse shaping in normally dispersive fibre systems.
Parabolic pulses in a ND two-segment fibre device

Tolerance to the length of the first fibre and influence of the initial chirp

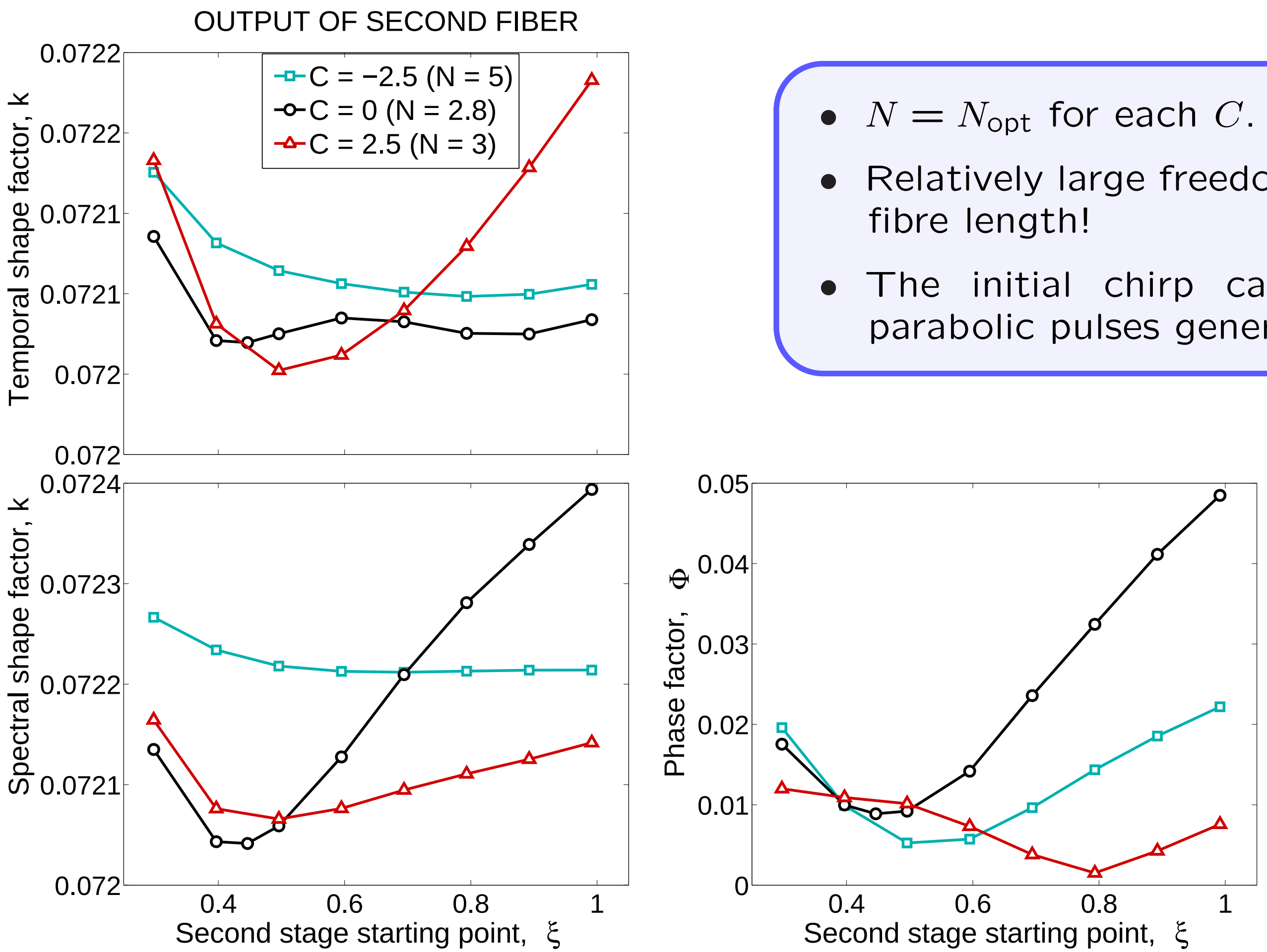

- $N = N_{\text{opt}}$ for each C.
- Relatively large freedom in the choice of the first fibre length!
- The initial chirp can be used to tailor the parabolic pulses generated in a ND fibre system!

S. Boscolo et al., IEEE J. Quantum Electron. (2008).

Photonic applications of pulse shaping

Parabolic pulses

- *High-power femtosecond lasers.*
- *Spectral broadening* and *supercontinuum generation.*
- *Nonlinear optical signal processing* and *regeneration.*

- J. Limpert et al., Opt. Express 10, 628 (2002).
- F. Ilday, F. Wise, and F. Kärtner, Opt. Express 12, 2731 (2004).
- B. Ortaç et al., Opt. Express 14, 6075 (2006).
- K. Tamura, H. Kubota, and M. Nakazawa, IEEE J. Quantum Electron. 36, 773 (2000).
- F. Parmigiani et al., Opt. Express 14, 7617 (2006).
- S. Boscolo and S. K. Turitsyn, IEEE Photon. Technol. Lett. 17, 1235 (2005).
- I. O. Nasieva, S. Boscolo, and S. K. Turitsyn, Opt. Lett. 31, 1205 (2006).

Flat-top pulses

- *Nonlinear optical switching* and *processing*.
- *Wavelength conversion.*

- P. Petropoulos et al., J. Lightwave Technol. 19, 746 (2001).
- F. Parmigiani et al., J. Lightwave Technol. 24, 357 (2006).
- J. H. Lee et al., Proc. of OFC, 200 (2003).
- T. Otani, T. Miyajaki, and S. Yamamoto, IEEE Photon. Technol. Lett. 12, 431 (2000).

Photonic applications of pulse shaping

Triangular pulses

- *Time-domain add-drop multiplexing.*
- *Wavelength conversion.*
- *Optical signal copying* and conversion of *time-domain to frequency-domain signal multiplexing.*

- J. Li et al., J. Lightwave Technol. 23, 2654 (2005).
- F. Parmigiani et al., Proc. of OFC, OMP3 (2008).
- A. I. Latkin, S. Boscolo, R. S. Bhamber, and S. K. Turitsyn, Phys. Rev. Lett. (2008), In preparation.
- R. S. Bhamber, A. I. Latkin, S. Boscolo, and S. K. Turitsyn, Opt. Lett. (2008), Submitted.

Applications of parabolic/flat-top pulses. All-optical signal regeneration

Regenerator scheme

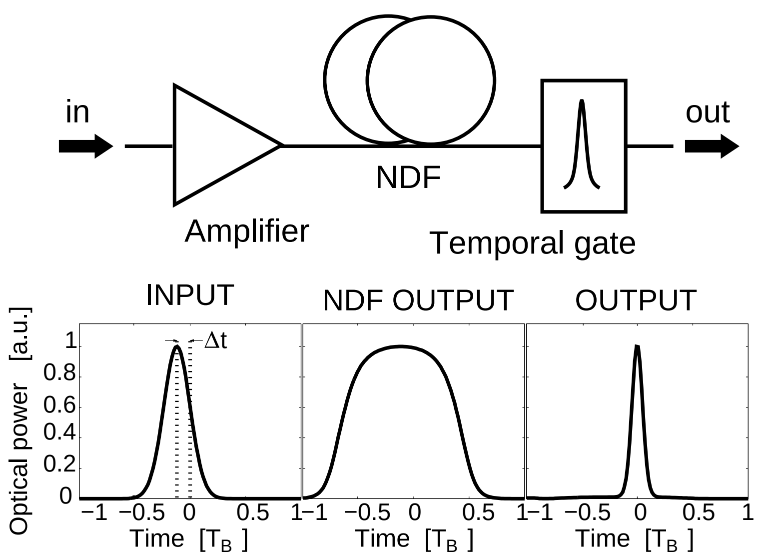

- *Nonlinear temporal pulse broadening and flattening* in a ND fibre +
  Subsequent *slicing of the pulse temporal waveform* by an optical temporal gate

  Efficient *suppression of the timing jitter* of a pulse train.

  S. Boscolo et al., IEEE Photon. Technol. Lett. (2005); Patent EP1834428 (2007), WO2006064240 (2006), GB2421382 (2006).

Example of temporal gate: Amplitude modulator with transfer function

$$f(t) = x + (1-x)\cos^{2m}[\pi(t-t_0)/T_B], \quad m = 1, 2, \ldots$$

– x: extinction ratio, t_0: center of the modulation, T_B: bit period. $m \Rightarrow$ Control of slicing of the pulse temporal profile.

$$f = f(t; m)$$

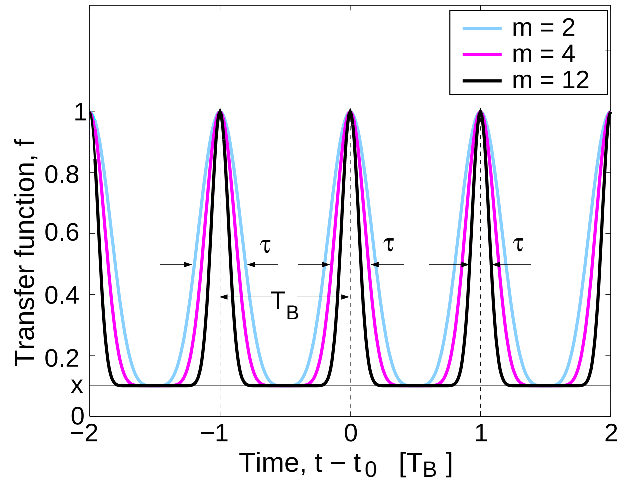

Regenerator performance at 40 Gbit/s bit rate

Timing jitter reduction

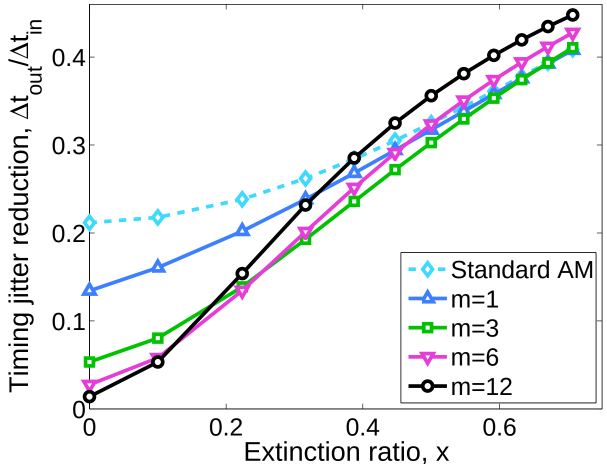

- Timing jitter: Average over the marks of standard RMS time position characteristics.

S. Boscolo et al., IEEE Photon. Technol. Lett. (2005).

Example of in-line application

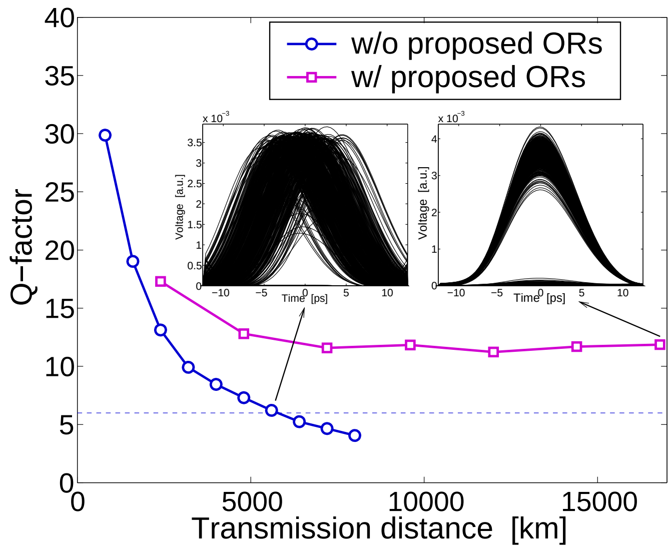

- Quality factor: $Q = |\mu_1 - \mu_0|/(\sigma_1 + \sigma_0)$,

  $\mu_{1,0}$, $\sigma_{1,0}$: mean and standard deviation of logical "ones" and "zeros".

- Stabilization of the timing jitter accumulation by the regenerators $\Rightarrow$ Q-factor stabilization.

Applications of parabolic/flat-top pulses.
Nonlinear optical signal pre-processing at the receiver

- Approach to the *bit-error rate (BER) improvement* utilizing a design of an advanced receiver enhanced by a nonlinear *all-optical decision element (ODE)*.

  I. O. Nasieva et al., Opt. Lett. (2006);
  S. K. Turitsyn and S. Boscolo, in: Dissipative Solitons: From Optics to Biology and Medecine, Lecture Notes Phys. 751 (Springer, 2008), 195.

Receiver scheme

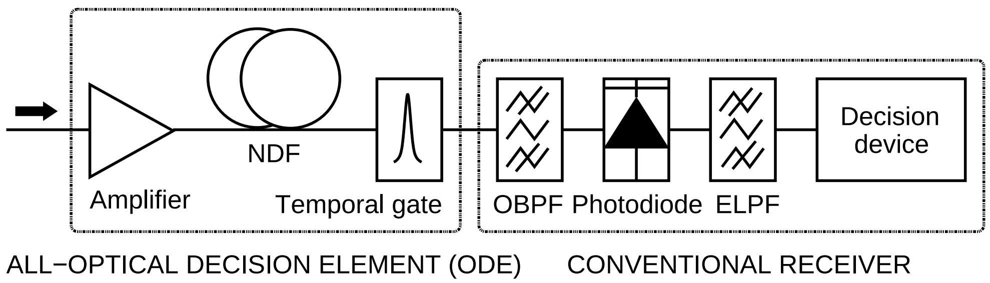

Decision in the optical domain based on *different information* from that used in the *electrical domain* ⇒ *Intrinsic BER improvement* by an optical device.

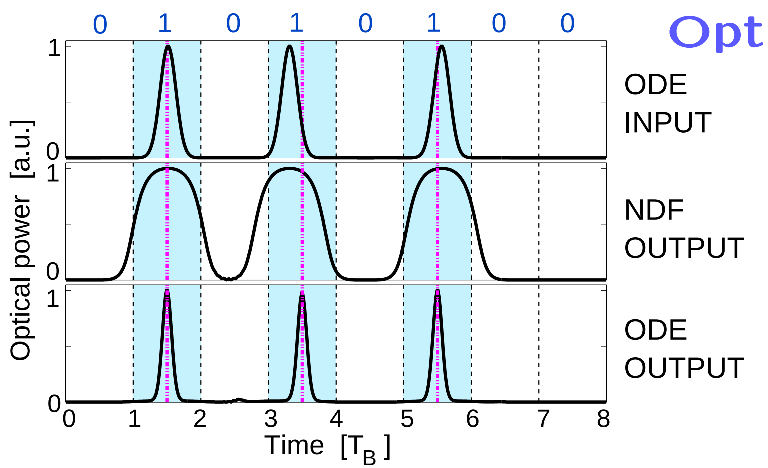

Optical decision scheme

- Temporal broadening and flattening-induced bit slot recovery in the ND fibre $\Rightarrow$ *Improvement of the BER*.
- Timing jitter suppression $\Rightarrow$ *Improvement of the receiver sensitivity*.

Applications of parabolic/flat-top pulses.
Nonlinear optical signal pre-processing at the receiver

Receiver performance at 40 Gbit/s bit rate

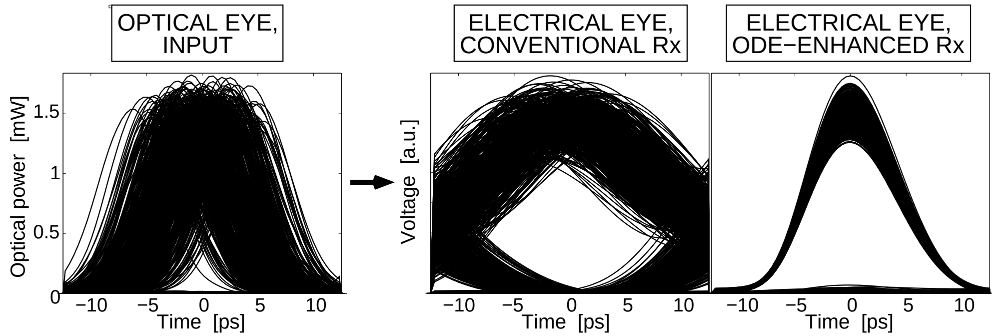

Signal quality

S. Boscolo et al.,
Opt. Express 13, 6217 (2005).

BER performance

- Multicanonical Monte Carlo method used.
- Input timing jitter standard deviation = 3 ps.
- BER = 4×10^{-4} for the conventional Rx
  BER = 10^{-5} for the ODE-enhanced Rx.

I. O. Nasieva et al., Opt. Lett. (2006).

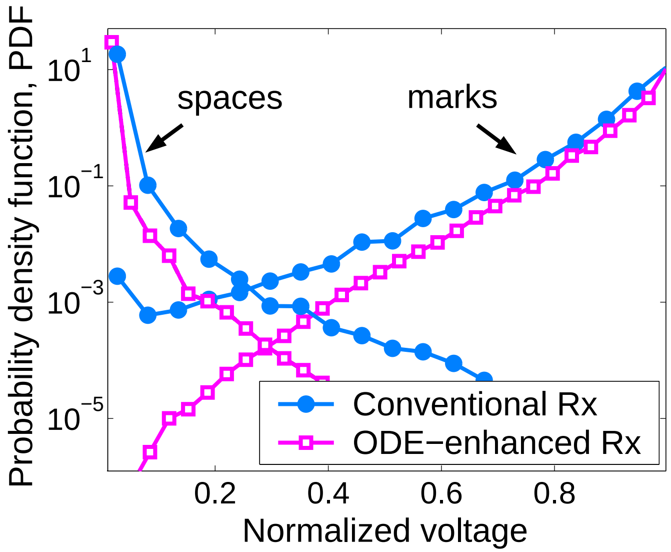

Applications of triangular pulses. Optical signal copying

- *Cross-phase modulation (XPM)* with a *triangular pump pulse* in a highly nonlinear (HNL) fibre + Subsequent *propagation in a dispersive medium*

$\Rightarrow$ Optical *pulse copying in time and frequency domains.*

A. I. Latkin et al., Proc. of ECOC (2008).

SPECTRAL COPYING

BACKGROUND. XPM interaction between two copropagating pulses with nonoverlapping spectra.

$$\psi_{1z} + \frac{i\beta_{21}}{2}\psi_{1tt} = i\sigma_1(|\psi_1|^2 + 2|\psi_2|^2)\psi_1, \quad \psi_{2z} + d\psi_{2t} + \frac{i\beta_{22}}{2}\psi_{2tt} = i\sigma_2(|\psi_2|^2 + 2|\psi_1|^2)\psi_2,$$

where $t = t - z/v_{g1}, \; d = (v_{g1} - v_{g2})/(v_{g1}v_{g2})$.

– v_{gj}, β_{2j}, σ_j: group velocity, GVD, and nonlinear coefficients of the two optical fields.

- Case $L \ll \tau_j/|d|$ and $L \ll \tau_j^2/|\beta_{2j}|$ (L: fibre length, τ_j: pulse widths).
- Pump-probe configuration: $P_1 \ll P_2$ (P_j: pulse peak powers).

$$\Downarrow$$

NLSE of signal pulse: $\psi_{1z} \approx i\sigma(2|\psi_2|^2)\psi_1$

$$\Downarrow$$

$$\psi_1(L,t) = \psi_1(0,t)\exp(i\phi), \quad \phi(L,t) = 2\sigma L|\psi_2(0, t - \delta t)|^2$$

(δt: initial relative time delay).

Applications of triangular pulses. Optical signal copying

$$\psi_1(0,t) = \sqrt{P_1}\exp(-t^2/(2T^2)), \quad \psi_2(0,t) = \sqrt{P_2}(1-|t/\tau|)^{1/2}\theta(\tau-|t|)$$
$$\Downarrow$$
$$\phi(t) = \phi_0(1-|t/\tau|)\theta(\tau-|t|), \quad \phi_0 = 2\sigma P_2 L,$$

$$\tilde{\psi}_1(\omega) = \psi_0(\omega)\exp(-\omega^2T^2/2) + \psi_-(\omega)\exp(-(\omega+\omega_0)^2T^2/2) + \psi_+(\omega)\exp(-(\omega-\omega_0)^2T^2/2),$$

where

$$\psi_0(\omega) = \sqrt{\pi/2}\sqrt{P_1}T\left[2 + \mathrm{erf}((i\omega T - \eta^{-1})/\sqrt{2}) - \mathrm{erf}((i\omega T + \eta^{-1})/\sqrt{2})\right],$$
$$\psi_-(\omega) = \sqrt{\pi/2}\sqrt{P_1}T\left[\mathrm{erf}((i(\omega+\omega_0)T + \eta^{-1})/\sqrt{2}) - \mathrm{erf}(i(\omega+\omega_0)T/\sqrt{2})\right],$$
$$\psi_+(\omega) = \psi_-(-\omega), \quad \eta = T/\tau, \quad \omega_0 = \phi_0/\tau.$$

A. I. Latkin et al., Phys. Rev. Lett. (2008).

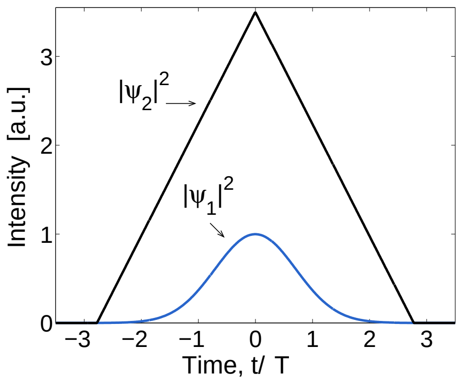

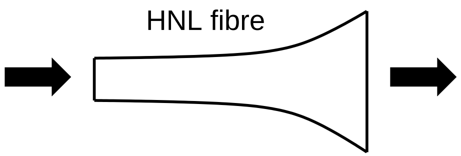

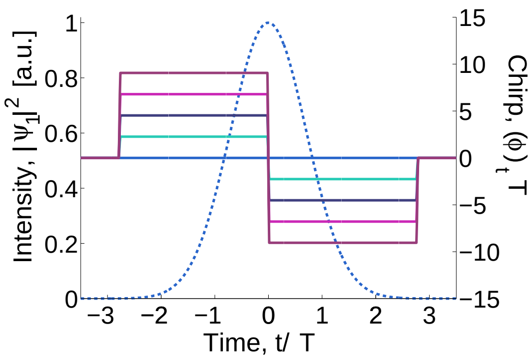

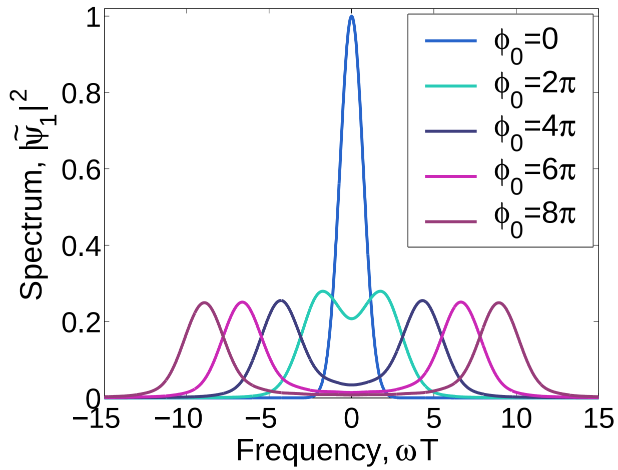

- $\eta = 0.36$.

TEMPORAL COPYING

Normal dispersion regime ($\beta_2 > 0$)

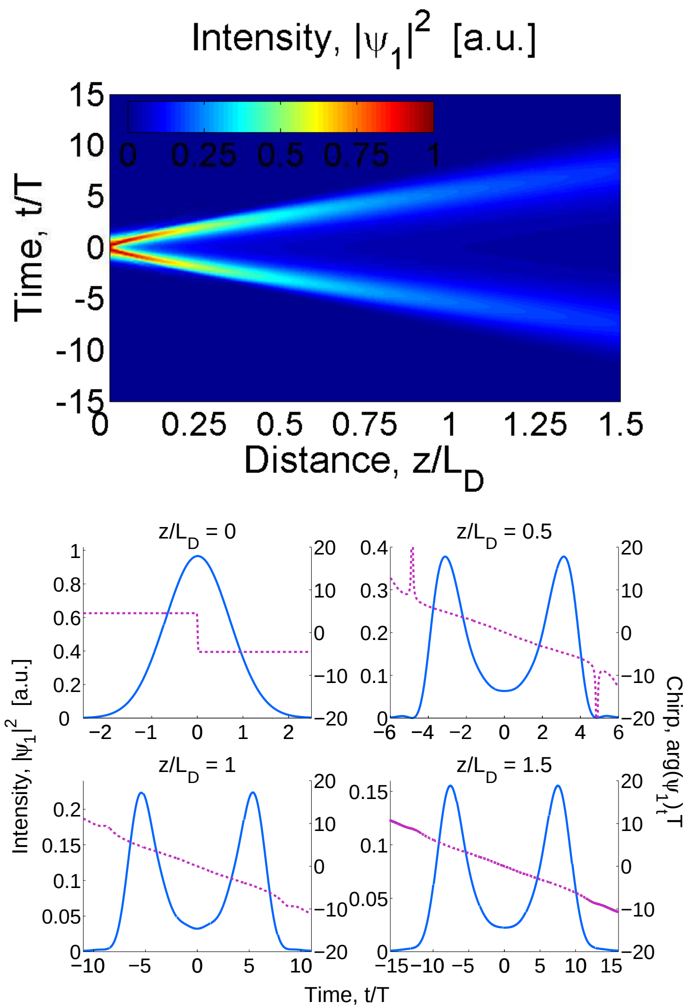

Propagation in linear dispersive medium:

$$\psi_1(z,t) = (2\pi)^{-1} \int d\omega\, \tilde{\psi}_1(0,\omega) \exp(i\beta_2\omega^2 z/2 - i\omega t).$$

– $\tilde{\psi}_1(0,\omega)$: modulated spectral amplitude at the HNL fibre output, β_2: GVD coefficient.

Anomalous dispersion regime ($\beta_2 < 0$)

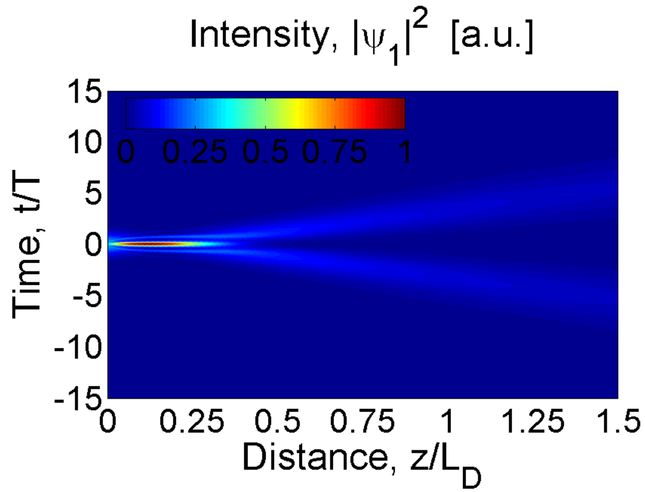

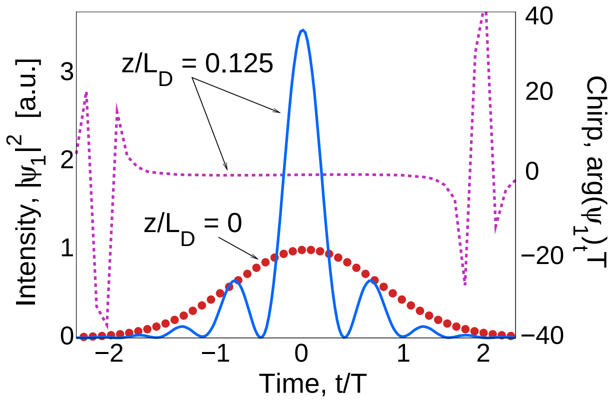

- $\eta = 0.36$, $\phi_0 = 4\pi$.

A. I. Latkin et al., Phys. Rev. Lett. (2008).

Applications of triangular pulses.
Time-to-wavelength mapping of multiplexed signals

- *XPM* in fibre with a *triangular pump pulse train*

⇩

Conversion of optical time-division multiplexed (TDM) signals to wavelength-division multiplexed (WDM) signals.

R. S. Bhamber et al., Opt. Lett. (2008).

Scheme of the TDM-WDM converter

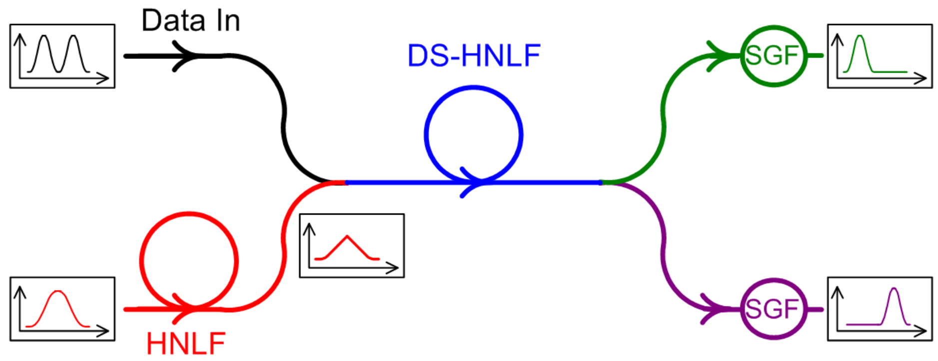

Pulse reshaping in the HNL fibre

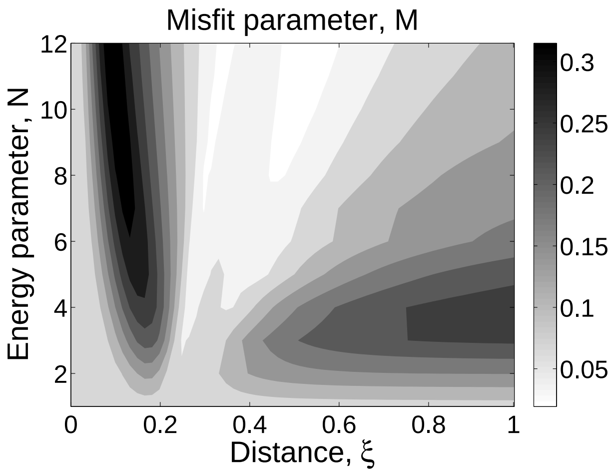

- $\psi(0,t) = \sqrt{P_0}\,\exp(-t^2/(2T^2) + iCt^2)$, $CT^2 = 2$.
- $M^2 = \int \mathrm{d}t\,(|\psi|^2 - |\psi_T|^2)^2 / \int \mathrm{d}t\,|\psi|^4$, $|\psi_T(t)|^2 = P_{0,T}(1 - |t/\tau|)\theta(\tau - |t|)$.
- $\xi = \beta_2 z/T^2$, $N = (T^2\sigma P_0/\beta_2)^{1/2}$.

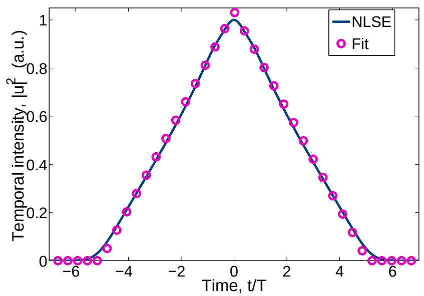

- $N = 10$, $\xi = 0.33$.

Applications of triangular pulses.
Time-to-wavelength mapping of multiplexed signals

Signal and pump at the DS-HNL fibre input

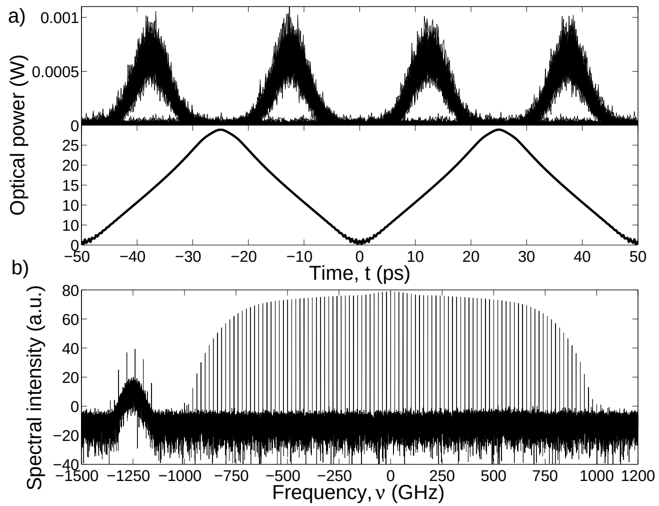

- Signal: return-to-zero amplitude-shift keyed pulse train at $B = 40\,\text{Gbit/s}$ ($T_b = 1/B = 25\,\text{ps}$). $\lambda_{0,S} = 1540\,\text{nm}$.
  Addition of noise.
- Pump: triangular pulse train at $20\,\text{Gbit/s}$. $\lambda_{0,T} = 1550\,\text{nm}$.
- Time delay $\delta t = T_b/2$.

XPM induced by the triangular pulses $\Rightarrow$ $\phi(t) = 2\sigma L \sum_n |\psi_{T,n}(t - 2nT_b - T_b/2)|^2$
($\psi_{T,n}$: triangular pulse amplitudes).

Signal at the DS-HNL fibre output

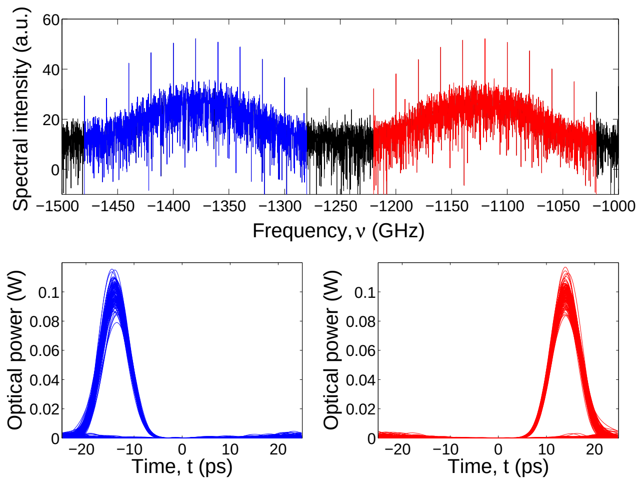

- Two WDM channels centered on $\lambda_{1,2} = \lambda_{0,S} \pm \delta\lambda$ and at $B/2 = 20\,\text{Gbit/s}$.
- Partial signal regeneration due to SPM + optical filtering.

R. S. Bhamber et al.,
Opt. Lett. (2008).

Summary

Examples of models and techniques for the *nonlinear optical pulse transformations* in *optical fibre systems*.

- Evolution of optical pulses in fibre lines with nonlinear optical devices as a *mapping problem*.
- *Generation and characterization of parabolic pulses* in active and passive fibres.
- *Passive nonlinear pulse shaping* in normally dispersive fibre systems.
- Applications of the parabolic/flat-top pulses in *nonlinear all-optical signal regeneration and pre-processing at the receiver*.
- Application of the triangular pulses in *optical signal copying* and *time-to-wavelength mapping of multiplexed signals*.